



Published in final edited form as:

Clin Cancer Res. 2009 April 15; 15(8): 2602–2611. doi:10.1158/1078-0432.CCR-08-2755.

Protumorigenic Role of HAPLN1 and Its IgV Domain in Malignant Pleural Mesothelioma

Alla V. Ivanova¹, Chandra M.V. Goparaju¹, Sergey V. Ivanov¹, Daisuke Nonaka¹, Christina Cruz¹, Amanda Beck¹, Fulvio Lonardo², Anil Wali², and Harvey I. Pass¹

¹Department of Cardiothoracic Surgery, Langone School of Medicine, New York University, New York, New York

²Department of Pathology, Karmanos Cancer Institute, Detroit, Michigan

Abstract

Purpose—Tumor extracellular matrix (ECM) plays a crucial role in cancer progression mediating and transforming host-tumor interactions. Targeting the ECM is becoming an increasingly promising therapeutic approach in cancer treatment. We find that one of the ECM proteins, HAPLN1, is overexpressed in the majority of mesotheliomas. This study was designed to characterize the protumorigenic role of HAPLN1 in mesothelioma.

Experimental Design—Overexpression of HAPLN1 was assessed and validated on a large set of normal/mesothelioma specimens on the RNA and protein levels. We also analyzed DNA copy number alterations in the HAPLN1 genomic locus using the array-based comparative genomic hybridization representational oligonucleotide microarray analysis tool. Tumorigenic activities of the HAPLN1 domains were evaluated *in vitro* on mesothelioma cells transfected with HAPLN1-expressing constructs.

Results—We found that HAPLN1 is 23-fold overexpressed in stage I mesothelioma and confirmed it for 76% samples ($n = 53$) on RNA and 97% ($n = 40$) on protein levels. The majority of lung cancers showed no differential expression of HAPLN1. Analysis of DNA copy number alterations identified recurrent gain in the 5q14.3 HAPLN1 locus in ~27% of tumors. Noteworthy, high expression of HAPLN1 negatively correlated with time to progression ($P = 0.05$, log-rank test) and overall survival ($P = 0.006$). Proliferation, motility, invasion, and soft-agar colony formation assays on mesothelioma cells overexpressing full-length HAPLN1 or its functional domains strongly supported the protumorigenic role of HAPLN1 and its SP-IgV domain.

Conclusion—Overexpression of HAPLN1 and its SP-IgV domain increases tumorigenic properties of mesothelioma. Thus, targeting the SP-IgV domain may be one of the therapeutic approaches in cancer treatment.

Malignant pleural mesothelioma (MPM) is a rare asbestos-associated malignancy of the pleura with a very poor prognosis. Conventional treatments for MPM such as surgery, chemotherapy, and radiotherapy have limited efficacy. MPM rarely metastasize to distant sites but are highly proliferative and locally invasive tumors that aggressively fill out pleural cavity, destroy normal lung structure, and result in high morbidity. Identification of biomarkers that could detect early-stage mesothelioma as well as an understanding of their

© 2009 American Association for Cancer Research.

Requests for reprints: Alla V. Ivanova, Vanderbilt-Ingram Cancer Center, Department of Hematology/Oncology, 648 PRB, 2220 Pierce Avenue, Nashville, TN 37232. alla.ivanova@vanderbilt.edu.

Disclosure of Potential Conflicts of Interest

No potential conflicts of interest were disclosed.

significance for tumor development and progression could help to develop effective early diagnostic and therapeutic tools for the disease.

In a recent study, we identified an important early marker of mesothelioma, osteopontin (OPN1), via RNA microarray analysis of stage I mesothelioma tumors (1). In the same set, we identified a yet another gene, hyaluronan- and proteoglycan-linked protein 1 (HAPLN1), which was highly expressed in tumors compared with normal mesothelium.

HAPLN1, which is also known as cartilage link protein (2), CRTL1, or link protein, is a 354-amino acid glycoprotein. It belongs to the link protein gene family that consists of four HAPLN members (3). All four link proteins show similar structure, with NH₂-terminal signal sequence followed by immunoglobulin-like domain and two link modules or proteoglycan tandem repeats. Other proteins that contain two adjacent link modules include extracellular matrix (ECM) proteoglycans aggrecan, brevican, neurocan, and versican. Tumor necrosis factor-inducible protein TSG-6 and cell surface antigen CD44 possess a single link module (4). All proteoglycan tandem repeats, or link modules, mediate binding to hyaluronic acid (HA).

Serving as a major component of cartilage ECM, HAPLN1 stabilizes aggregates of aggrecan and HA (5). In the absence of HAPLN1, aggregates are smaller and less stable (6). HAPLN1 binds aggrecan along the HA chain with a 1:1 stoichiometry. The resulting aggregates are entrapped within the mesh-like network of type II collagen fibrils producing a large stable macromolecular structure that contributes to compression resistance and shock absorption in the joint (6).

Although HAPLN1 is a major component of cartilage ECM, it is also highly expressed in noncartilaginous tissues such as small intestine and placenta (3), embryonic and adult heart tissues (7), and, to a lower extent, many other tissues.

Expression of HAPLN1 in cancers and its significance for tumorigenesis have not yet been addressed in spite of its capacity to interact with HA, an abundant component of many tumors (8–11), tumor ECM (12), and urine of cancer patients (13). It has been well known that HA receptors and HA-binding proteins are involved in tumor growth and metastasis in various cancer tissues via regulation of cell cycle, gene transcription, or modulation of cell signaling (14–21). High HA levels are also typical for most cases of mesothelioma. *In vitro* experiments have shown that HA overproduction increases the malignant properties of MPM cells (22). In >70% of MPM cases, elevated levels of HA have been found in the pleural fluid and in serum (23–25). The major cell surface receptor for HA, CD44H, was shown to be present in 75% of MPM and 100% cases of reactive mesothelium (24, 26).

Our expression microarray analysis of MPM specimens and matched normal healthy peritoneum controls revealed a ~23-fold overexpression of HAPLN1 in tumors. This finding was supported by semiquantitative reverse transcription-PCR (RT-PCR) analysis and identification of a gain in the 5q14.3 chromosomal area where HAPLN1 is localized. Functional assays that we performed on MPM cells overexpressing HAPLN1 augmented tumorigenic pathways such as proliferation, motility, invasion, and anchorage-independent colony formation. We also created a series of HAPLN1 deletion constructs to identify HAPLN1 domains essential for tumorigenic activities. We found as a result that HAPLN1 domains may possess distinct and even opposite effects on MPM cells tumorigenicity.

Overall, our data suggest that activation of HAPLN1 expression modulates mesothelioma behavior *in vitro*, which may explain differences in the aggressiveness of individual tumors.

Materials and Methods

Mesothelioma and lung cancer specimens and RNA isolation

All patients gave informed consent for deidentified use of tissues under the Wayne State University institutional review board-approved tissue consent document D1420: Collection of Serum and Tissue Samples for Patients with Biopsy-Proven or Suspected Malignant Disease. Immediately after surgical resection, tissues were snap frozen and kept at -80°C until RNA isolation. RNA was isolated using Ambion RNA extraction kit. Affymetrix U133Plus2 microarray analysis was done using RNA from snap-frozen specimens (8 normal peritoneum and 7 stage I mesotheliomas), with analysis in refs. 27–29. Validation by RT-PCR analysis was done on RNA isolated from 35 paired normal peritoneum/mesothelioma tissues, 14 nonpaired mesotheliomas, 9 nonpaired normal peritoneum, and 52 paired normal lung/lung cancer tissues. Immunostaining with anti-HAPLN1 antibodies was done on tissue microarray slides including 40 mesothelioma samples and 60 lung cancer samples. For representational oligonucleotide micro-array analysis (ROMA) analysis, 27 snap-frozen specimens (22 tumors and 5 normal tissues) derived from 22 patients with MPM were used to produce 27 DNA samples. Four of 5 normal samples were tumor-matched. DNA from snap-frozen tissues was isolated with QIAamp mini-kit (Qiagen) and assayed for concentration and quality using Victor3 microplate reader (Perkin-Elmer). All of these 27 samples for ROMA analyses, including one other mesothelioma sample, had previously undergone expression analyses done using the Affymetrix U133A platform and were available for analysis of HAPLN1 expression (probe ID 205523_at). Complete demographics, including time to progression and survival, were available for all 23 mesothelioma specimens.

ROMA and data processing

Arrays were described previously (30). ROMA and all data processing procedures were done as described in ref. 31.

RT-PCR analysis

RT-PCR premixes were prepared using SuperScript One-Step RT-PCR kit (Invitrogen). We used 25 ng total RNA/20 mL reaction volume for RT-PCR. Primers for RT-PCR assessment of gene expression were designed as described (32). Conditions for the reaction were as follows: 50°C for 30 min and 35 cycles of (94°C for 15 s, 56°C for 15 s, and 72°C for 1 min) 72°C for 5 min. Oligonucleotide sequences for RT-PCR of HAPLN1 were designed to ensure RNA-specific synthesis across introns ($5'$ -TCTCCAGCTTCCAACCTAAGC- $3'$ and $5'$ -TGCTGCGCCTCGTGAAAATTGAG- $3'$). RT-PCR with primers to invariantly express PPIA ($5'$ -TCTGAGCACTGGAGAGAAAGG- $3'$ and $5'$ -GGAAAACATGGAACCCAAAGG- $3'$) was used as a loading control. RT-PCR was done on a set of matched normal-tumor specimens from 25 MPM patients. Band intensities were measured using Kodak 4000 Image Station. Repeated experiments showed consistency of our RT-PCR analysis.

Immunofluorescent staining of cultured cells

Cells were cultured on coverslips overnight. In the morning, cells were fixed with 3% paraformaldehyde for 30 min and permeabilized with 0.1% Triton X-100 for 5 min. After preincubation with 1% fetal bovine serum (FBS), cells were incubated with primary anti-HAPLN1 (1:200) at room temperature for 1 h. This was followed by incubation with anti-rabbit Alexa Fluor-conjugated secondary antibodies (Molecular Probes). Cells were mounted in mounting medium containing 4',6-diamidino-2-phenylindole (Vector Laboratories).

HAPLN1 immunostaining of tissue microarray slides

For immunohistochemistry, tissue microarrays sections were deparaffinized in xylene (three changes), rehydrated through graded alcohol (three changes of 100% ethanol and three changes of 95% ethanol), and rinsed in distilled water. Heat-induced epitope retrieval was done by microwave boiling in 10 mmol/L citrate buffer (pH 6.0) for 20 min. The sections were allowed to cool down to room temperature for 30 min, rinsed in distilled water, and blocked for endogenous peroxidase with 3% H₂O₂. For HAPLN1 detection, we used rabbit anti-HAPLN1 polyclonal antibody directed against the 20-amino acid epitope (Genosis) and avidin-biotin enzyme complex kit (LSAB2; DAKO). All sections were incubated with primary antibody at a 1:200 dilution overnight at 4°C, with biotinylated secondary linking antibody for 30 min, streptavidin-enzyme complex for 30 min, and diaminobenzidine as chromogen for 10 min. Nuclei were lightly counterstained with hematoxylin, and slides were hydrated and mounted with permanent medium. We used rabbit IgG as a negative control.

Histologic assessment

Immunohistochemical staining was evaluated by one of the authors (D.N.) and the results were scored semiquantitatively based on the percentage of positive cells present in the total field of a single section. Immunohistochemical analysis of HAPLN1 was scored as follows: 0, no staining; 1+, 1% to 25% tumor cells reactive; 2+, 25% to 50% tumor cells reactive; 3+, 50% to 75% tumor cells reactive; and 4+, 75% tumor cells reactive.

Cell lines

Mesothelioma cell lines were grown in 1× DMEM supplemented with sodium pyruvate and high glucose and 10% FBS (Invitrogen). All mesothelioma cell lines in the study but Hmeso were established in our laboratory from the surgical specimens of Dr. Pass (33). Hmeso cell line was obtained from the American Type Culture Collection.

HAPLN1 and its deletion mutants overexpressing constructs and transfection

The constructs for expression of the human HAPLN1 and its deletion mutants were obtained by RT-PCR from the plasmid expressing HAPLN1 (OriGene). The amplified products were TA cloned, excised with *EcoRI* and *XhoI*, and subcloned into the pCMV2/FLAG vector (Sigma-Aldrich). Genes cloned into this vector are expressed under the control of the CMV promoter. Sequence fidelity and accurate reading frame were verified by DNA sequencing analysis. All cells in the study were transfected using Lipofectamine 2000 (Invitrogen) according to the manufacturer's protocol.

Cell proliferation assay

Transfected cells (3×10^3) in 100 μ L DMEM/10% FBS were plated in flat-bottomed 96-well plates in six replicates and incubated at 37°C for 48 h. Then, 20 μ L Cell Titer-Blue reagent (Promega) was added to each well (containing 100 μ L cell culture medium) and incubated for another 1 to 3 h at 37°C. Absorbance value was measured at 560/590E using the Universal Reader Victor³ (Perkin-Elmer Life and Analytical Sciences).

Scratch assay (wound closure assay)

Cells (2×10^5 per well) were seeded into 6-well plates 24 h before the experiment. Two to three scratches per well were done using 1 mL pipette tip and medium was changed after scratching to avoid conditioning of the medium with floating cells. Scratched areas were marked on a plate with fine pointer. The scratch width (6–9 measurements per well) was measured right after scratching and 16 h later and the percentage of the scratch closure, reflecting the motility rate, was calculated.

Cell invasion assays

Cell invasion assay was done using the BD Biocoat Matrigel Invasion Chambers in accordance with the manufacturer's protocol. Cells (1×10^5 /mL) were seeded onto 12-well cell culture chamber using inserts with 8 μ m pore size polycarbonate membrane over a thin layer of Matrigel Basement Membrane Matrix without phenol red (BD Biosciences) diluted at 1:100 in PBS. Following incubation of the plates for 48 h at 37° C, cells that invaded through the Matrigel and migrated to the lower surface of the membrane were stained with Giemsa solution, counted under the microscope in at least 10 different fields, and photographed. Three wells were examined for each condition and cell type, and the experiments were repeated in triplicate.

Soft-agar colony formation assay

Plates with base agar were prepared 30 min before cell plating as follows: equal volumes of 1% agarose at 40 °C and warm 2 \times DMEM/10% FBS are mixed up, poured into a plate (1.5 mL/well in 6-well plate), and left to harden. Cells (5×10^3) were mixed with warm 0.35% agarose in DMEM/10% FBS and immediately poured on the base agar. Plate were incubated at 37°C in humidified incubator for 10 to 14 days, and colonies were stained with 0.5 mL 0.005% crystal violet for >1 h and counted using a dissecting microscope.

Statistical analysis

The HAPLN1-dependent changes from all functional assays were analyzed for statistically significant differences by the Student's t test, accepting a probability of error of <5%. Kaplan-Meier survival plots and log-ranktests were used to assess differences between high and low HAPLN1 expressors using MedCalc Software.

Results

HAPLN1 is overexpressed in the majority of mesotheliomas

Transcriptional profiles of 8 normal peritoneum samples and 7 stage I MPM specimens were established using Affymetrix microarray U133 plus platform followed by an unsupervised clustering analysis of microarray data. We found a clear segregation of normal pleura and malignant samples based on the analysis of overexpressed and underexpressed genes. Previously, we reported that one of the highly overexpressed (~17-fold) genes, osteopontin (OPN1), is a potential serum-based MPM early detection marker (1). Expression of the HAPLN1 gene in the same set of tumors was found to be ~23-fold higher than in normal peritoneum (Fig. 1A). We validated these data by real-time RT-PCR analysis on RNA isolated from the same set of samples that were used for the microarray analysis (data not shown).

We used a larger set of unmatched and matched normal peritoneum/malignant mesothelioma samples to confirm these results by RT-PCR analysis. Analysis of HAPLN1 expression in 31 paired and 23 unpaired clinical samples showed that HAPLN1 was overexpressed in 76% of mesothelioma samples (Fig. 1B). We found that the level of HAPLN1 expression is pronounced in all stages and in all histologic types of MPM. To find out whether HAPLN1 overexpression is specific to MPM, we analyzed its expression in a large set of matched clinical lung cancer samples consisting of 21 lung adenocarcinomas, 18 squamous cell carcinomas, 3 non-small cell lung cancer, and 9 bronchioloalveolar lung cancers. We found no tumor-specific increase in HAPLN1 expression in any of these lung cancer types (Fig. 1B), allowing us to suggest that, of all thoracic malignancies, HAPLN1 overexpression is highly specific to malignant mesotheliomas.

HAPLN1 is the only gene from the link protein gene family that is overexpressed in mesothelioma

HAPLN1 belongs to a linkprotein gene family (*HAPLN*), consisting of four members (HAPLN1, HAPLN2, HAPLN3, and HAPLN4). The sequence conservation of these genes between vertebrate species is very high, reflecting the fundamental importance of their function in vertebrate species (3). Analysis of the expression of HAPLN genes in normal tissues suggested tissue-specific constraints for most of them because HAPLN1 was predominantly expressed in small intestine and placenta, HAPLN2 and HAPLN4 was expressed in brain, and only HAPLN3 showed near ubiquitous but low expression (3). We performed RT-PCR analysis of HAPLN2, HAPLN3, and HAPLN4 on the same panel of matched mesothelioma samples (Fig. 1B). The experiment showed that HAPLN1 is the only member of the gene family expressed in mesothelioma (Fig. 1C), suggesting its specific role in mesothelioma.

The HAPLN1 locus is frequently amplified in MPM tumors

Increased HAPLN1 expression in ~75% of mesotheliomas prompted us to seek possible mechanism(s) of its up-regulation. Because amplification of genomic regions is a frequent event in cancer, we used our previously reported ROMA (31) to find out whether the 5q14.3 locus containing the HAPLN1 gene (pos. 82972493–83052454) is the subject of copy number alteration in mesotheliomas. ROMA copy number alteration data generated on 22 tumor specimens were processed using the analysis of copy errors algorithm available from CGH Explorer³ and plotted across chromosome 5 (Fig. 1D). We found that a ~2 MB of the HAPLN1-containing 5q14.3 region was amplified in 6 of 22 (~27%) analyzed samples, suggesting that 5q14.3 gain is one of the mechanisms that may increase HAPLN1 expression in mesotheliomas.

Specificity of HAPLN1 antibodies and assessment of intracellular and intratumoral localization of the HAPLN1 protein

We generated affinity-purified rabbit HAPLN1 polyclonal antibodies against a 20-amino acid immunogenic human HAPLN1 peptide and compared the affinity and specificity of these antibodies with the commercially available mouse monoclonal anti-HAPLN1 antibody (R&D Systems). We used human recombinant HAPLN1 protein (R&D Systems) for Western blot analysis and showed that both antibodies have an identical band pattern that was consistent with the molecular weights of the HAPLN1 products. Our rabbit affinity-purified antibodies, however, showed a higher sensitivity (Fig. 2A). Western blot with preimmune serum as a negative control did not produce any signal (data not shown). Immunofluorescent analysis of mesothelioma cell lines using rabbit anti-HAPLN1 antibodies showed a dotted cytoplasmic pattern of HAPLN1 protein distribution. MPM cells stained intensely, whereas normal mesothelial cell line Met5A showed only a weak signal if at all (Fig. 2B).

HAPLN1 protein is specifically overexpressed in mesotheliomas

We used both rabbit and mouse HAPLN1 antibodies to analyze expression of this protein in several clinical samples of MPM. Both antibodies produced similar staining patterns with rabbit antibodies, showing higher sensitivity to the HAPLN1 protein. All MPM types (epithelial, mixed, and sarcomatoid as well as reactive mesothelium) stained strongly with HAPLN1 antibodies. Lung parenchyma and adjacent normal pleura were HAPLN1-negative, whereas fibroblasts in the tumor-associated stroma, media, and intima of vessels were weakly positive (Fig. 2C).

As rabbit anti-HAPLN1 antibodies showed higher sensitivity, we used these antibodies to screen tissue microarray slides of MPM and lung cancer to confirm our data on HAPLN1 overexpression in mesothelioma on the protein level. Scoring of 40 stained MPM and 60 lung cancer specimens showed that the HAPLN1 protein level is highly elevated in the majority of MPM, with only one tumor specimen being HAPLN1-negative (Table 1). On the contrary, 53 (88%) lung cancer samples showed no HAPLN1 staining of the tumor components and 12% of lung cancers produced weak or moderate signals, which confirmed our finding that HAPLN1 overexpression is specific for MPM.

HAPLN1 expression is negatively correlated with time to progression and survival

We compared HAPLN1 expression in 23 MPM patients using gene expression profiling data produced on Affymetrix U133A platform. MPM patients were stratified into two groups based on the extent of HAPLN1 expression level (Fig. 3). Thirteen patients with higher level of HAPLN1 expression progressed within 1 year of surgery (Fig. 3A, *bottom curve*), whereas 10 patients that had low HAPLN1 level had tumor progressed later than 12 months after surgery ($P=0.05$, log-ranktest; Fig. 3A). HAPLN1 expression highly correlated with survival time for these patients as well ($P=0.006$, log-ranktest; Fig. 3B).

Overexpression of HAPLN1 augments proliferation, motility, invasion, and anchorage-independent growth of MPM cell lines

As increased proliferation, motility, invasion, and anchorage-independent growth are the hallmarks of tumorigenic potential, we compared these activities with or without transgenic HAPLN1 expression. MPM cell lines of different histologic origin, HP1 (biphasic) and H2595 (epithelial), were transiently transfected with a pCMV-based plasmid construct expressing the HAPLN1 gene and with control empty vector. Both cell lines showed low endogenous HAPLN1 levels of in our quantitative RT-PCR assessment (data not shown). Our preliminary studies also showed that sustained high level of exogenous HAPLN1 expression can be maintained in the transfected MPM cells for as long as 4 weeks after transfection, a period sufficient for all functional assays (data not shown).

We showed that HAPLN1 overexpression led to ~4- and ~1.7-fold increase in the proliferation rate of HP1 and H2595 cell lines, respectively (Fig. 4). We also performed two assays to study HAPLN1 metastatic potential, a wound closure assay that reflects changes in cell motility on two-dimensional surface, and a cell invasion assay that shows three-dimensional motility using Matrigel as an ECM. As can be seen in Fig. 4, both HP1 and H2595 cells prominently increased their motility rate on HAPLN1 expression. A dramatic increase in the invasive potential of HP1 and H2595 cells expressing HAPLN1 (5- and 10-fold, respectively) convincingly showed that the HAPLN1 protein promotes metastatic capability of these cells. The soft-agar colony formation assay showed that HAPLN1 increases H2595 cell anchorage-independent growth up to ~2.5-fold. HP1 cells that do not possess an innate ability to form colonies in soft agar did not attain this property on HAPLN1 overexpression. Thus, the HAPLN1 protein potently promotes innate tumorigenic abilities, including metastatic growth of mesothelioma cells *in vitro* but is not sufficient per se for the establishment of such tumorigenic characteristic as anchorage-independent growth *in vitro*.

Involvement of the HAPLN1 protein domains in regulation of tumorigenic properties

Proliferation, migration, and anchorage-independent growth—All four HAPLN proteins show similar structure defined by the NH₂-terminal signal sequence (SP) followed by the immunoglobulin domain (IgV) that is involved in a variety of functions, including cell-cell recognition and intracellular signaling, and two consecutive linkmodules (L) that mediate binding to HA (3). The immunoglobulin-like domain of the HAPLN1 protein was

found to interact with aggrecan stabilizing and promoting the interaction of aggrecan with HA (34, 35). We have analyzed the effect of each of the HAPLN1 domains on the tumorigenic properties of this protein. By removing these domains one by one, we created four protein expression constructs (Fig. 5A). We then transiently transfected these constructs into two epithelial mesothelioma cell lines, H2595 and Hmeso (Fig. 5B). We included Hmeso in our analysis because this cell line does not express HAPLN1 mRNA and possesses the unique ability to form abundant colonies in soft agar. Cells transfected with the HAPLN1 deletion constructs were compared with those transfected with empty vector (mock control cells).

Differences in the proliferating capacity between mock and HAPLN1 mutant-transfected cells were assessed by measuring cell density at 48 h on plating equal number of cells in 96-well plate. We found that cells transfected with the plasmids expressing the full-length HAPLN1 or SP-IgV mutant that lacks two link domains showed similarly moderate but steady increase in the proliferation ability compared with the mock-transfected cells (Table 2). Loss of the 33-amino acid NH₂-terminal peptide in the IgV-LL mutant negated the HAPLN1 stimulative effect on proliferation; further truncation of the protein from the NH₂ or COOH terminus (LL and SP-IgV-L mutants) led to a complete loss of proliferation function of the HAPLN1 exogenous protein (Table 2).

Likewise, in the motility assay, both the full-length HAPLN1 and the SP-IgV mutant increased similarly and significantly the motility of transfected cells, whereas all other mutants caused little or no effect (Table 2).

We then investigated the involvement of the HAPLN1 protein domains in the anchorage-independent cell growth. We showed that the SP-IgV mutant lacking both link domains still retained or even increased the ability to stimulate colony formation in soft agar compared with the intact HAPLN1 protein. However, the IgV-LL mutant that contains IgG and two link domains but lacks the NH₂-terminal signal sequence peptide loses this ability (Fig. 5C).

Interestingly, cells expressing the SP-IgV construct produced not only higher number of colonies but also larger colonies (Fig. 5C, *right*). The median diameter of the colonies formed in cells expressing the SP-IgV mutant was ~2.5-fold bigger than in cells transfected with empty vector (Table 2). Moreover, the shape of the colonies formed by SP-IgV-transfected cells was more irregular and spread out in different directions compared with round-shaped colonies from control cells (Fig. 5C, *right*). The full-length HAPLN1 also caused a slight but statistically significant increase (~25%) in colony size, whereas IgV-LL-transfected cells formed slightly smaller (~15%) colonies (Table 2). All other constructs did not affect the colony size.

HA modulates the invasive potential of the full-length HAPLN1 protein and its deletion mutants—HAPLN1 possesses two link domains implicated in binding to HA, which serves as a component present in ECM. To assess how HA added to growth medium may influence the HAPLN1 effects on MPM cells behaviors, we performed an invasion assay on cells transfected with the HAPLN1 deletion mutants. The invasion assay was chosen based on the recent reports on HA effects on cell invasion (36, 37). The ability to invade was assessed by migration through Matrigel toward the regular DMEM/FBS compared with HA-supplemented DMEM/FBS. We found that the already high invasive potential of the HAPLN1-transfected cells was further increased in the HA-supplemented medium. Thus, if HAPLN1-expressing H2595 cells in regular medium showed a ~2.5-fold increase in invasion compared with control cells, the same cells showed a ~4.0-fold increase in the medium supplemented with 50 mg/mL HA (Fig. 6). Surprisingly, we found the

opposite effect of HA on cells transfected with the SP-IgV mutant: whereas, in the regular medium, SP-IgV cells showed the invasive potential similar to that of HAPLN1-transfected cells, the HA-containing medium reduces their invasion ability from a ~2.5-fold increase to a ~1.6-fold increase (Fig. 6). As for the other mutants, the invasive potential of the IgV-LL mutant lacking signal sequence peptide was much lower than that of the intact HAPLN1 protein with or without HA. The remaining mutants, LL and SP-IgV-L, did not show any considerable effects compared with the control cells (Fig. 6).

These results suggest that whereas most of the HAPLN1 tumorigenic functions are mediated via the NH₂-terminal immunoglobulin domain of the HAPLN1 protein, the HA-promoted tumorigenic changes require the entire HAPLN1 molecule.

Discussion

The tumor microenvironment plays a key role in cancer progression. Specifically, HA-rich tumor microenvironments regulate important host-tumor interactions and have a significant effect on many aspects of cancer initiation and malignancy. The HA-rich microenvironment accelerates the recruitment of inflammatory cells, thus providing cytokines and chemokines for tumor growth and angiogenesis. As such, targeting ECM, a gel-like structure of HA polymers and hyaladherins at different stoichiometric ratios, is becoming an increasingly promising therapeutic approach to cancer treatment.

In this work, we first identified the HA-binding protein HAPLN1 as transcriptionally up-regulated in stage I MPM compared with healthy peritoneum and confirmed it on a large set of MPM specimens. Moreover, we associated differential HAPLN1 expression with chromosomal gain at 5q14.3 and up-regulation of HAPLN1 on the protein level (Figs. 1 and 2). Because HAPLN1 has never been implicated in MPM or any other cancers, our findings are original. Association of HAPLN1 overexpression with MPM but not lung cancers suggests a special role that HAPLN1 plays in the etiology of MPM. Moreover, analysis of HAPLN1 expression levels in MPM patients showed that high level of HAPLN1 is associated with fast progression and poorer survival, thus suggesting that HAPLN1 may be used as a prognostic marker.

Malignant progression of MPM is characterized by the acquisition of pathologic growth and invasive properties. Using assays evaluating malignant potential *in vitro*, we established that HAPLN1 increases tumorigenic abilities of all tested MPM cell lines. Interestingly, HAPLN1 served as an enhancer but not as an inducer of tumorigenic functions: in cells not capable of anchorage-independent growth, HAPLN1 did not induce this ability; however, in cells possessing this trait, such as Hmeso, HAPLN1 expression significantly enhanced the anchorage-independent growth ability (38).

It is known that HA regulates cell proliferation, migration, and invasion in both normal and pathologic environments (36, 37). In our experiment, we found that HA-supplemented medium augmented the invasive effect of the HAPLN1 protein, suggesting that HAPLN1 invasion-stimulatory effect depends on the presence of HA in the environment. Our observation that the HAPLN1 mutant (SP-IgV) lacking both link domains decreases its ability to invade in HA presence suggest that the full-length HAPLN1 protein is required to mediate its HA-dependent activities.

To dissect the effect of each of the HAPLN1 protein domains on its protumorigenic properties, we created a series of HAPLN1 truncations and tested their tumorigenic potential in the same set of functional assays. Interestingly, we observed that truncation of the NH₂-terminal 33 amino acids practically abrogates the protumorigenic properties of the HAPLN1 and further deletion of the protein from the NH₂ terminus led to complete negation of its

function. These data clearly showed that protumorigenic activities of the HAPLN1 are mediated through its NH₂ terminus. This notion was further confirmed by the set of experiments with the overexpression of the NH₂ terminus (SP-IgV) in mesothelioma cells, which mimicked and even augmented the protumorigenic properties of the full-length HAPLN1. These data strongly suggest that HAPLN1 protein owes its tumorigenic potential to the first 157 amino acids containing SP and IgV domains.

The IgV domain of HAPLN1 belongs to an immunoglobulin superfamily. Some members of this family are immunoglobulin-like cell adhesion molecules that have been implicated in cell-cell adhesion, tumor cell invasion, and metastasis (39, 40). The IgV domain of HAPLN1 binds aggrecan and versican in ECM (41), whereas the link domains bind to HA (42). In addition to providing mechanical cell-cell and cell-ECM adhesion, they also activate signaling receptors and induce intracellular signaling cascades (43). By dissociating the IgV domain from the linkdomains, we created the molecule that was incapable of HA binding and HA-dependent functions. MPM cells overexpressing SP-IgV showed a high invasive capability that was drastically decreased in the HA-containing medium. On the other hand, the SP-IgV mutant was still capable to promote the protumorigenic functions, suggesting that the NH₂-terminal part of the protein is intimately involved with the tumorigenic potential of the HAPLN1 molecule. The mechanism of the antitumorigenic effect of the constructs lacking the NH₂-terminal peptide of the HAPLN1 protein is currently unknown. One possibility is that the HA-binding activities of the IgV-LL antagonize constitutive interaction of HA and CD44, blocking the protumorigenic activity of the HA and CD44 complex. On the other hand, the inactive isoform of HAPLN1 may act as a decoy for the protumorigenic HAPLN1 protein, displacing it from its native ECM environment and disrupting HAPLN1-mediated tumorigenic signaling. Compounds capable of competing with HA in its interaction with CD44 have been characterized as antitumorigenic agents. Such compounds include HA oligomers or soluble HA-binding proteins: soluble CD44, RHAMM, and the brevicin linkmodule (38, 44–48).

It will be of considerable interest to determine whether perturbation of the hyaluronan meshwork on mesothelioma cells by overexpression of inactive HAPLN1 inhibits mesothelioma progression *in vivo*. Also, it would be of great interest to investigate which amino acids of the SP-IgV HAPLN1 domain are crucial for the promotion of its tumorigenic activity and whether disruption of these active sites will reduce the HAPLN1 tumorigenic potential.

Finally, as an ultimate goal, we would like to learn whether interventions based on these approaches might provide useful therapies in mesothelioma patients.

Acknowledgments

Grant support: Early Detection Research Network National Cancer Institute/NIH grant 5 U01 CA111295-02, Mesothelioma Applied Research Foundation, Department of Veterans Affairs Merit Review Award, and Belluck & Fox, LLP.

References

1. Pass HI, Lott D, Lonardo F, et al. Asbestos exposure, pleural mesothelioma, and serum osteopontin levels. *N Engl J Med.* 2005; 353:1564–1573. [PubMed: 16221779]
2. Neame PJ, Christner JE, Baker JR. The primary structure of link protein from rat chondrosarcoma proteoglycan aggregate. *J Biol Chem.* 1986; 261:3519–3535. [PubMed: 2419334]
3. Spicer AP, Joo A, Bowling RA Jr. A hyaluronan binding link protein gene family whose members are physically linked adjacent to chondroitin sulfate proteoglycan core protein genes: the missing links. *J Biol Chem.* 2003; 278:21083–21091. [PubMed: 12663660]

4. Barta E, Deak F, Kiss I. Evolution of the hyaluronan-binding module of link protein. *Biochem J.* 1993; 292:947–949. [PubMed: 8318021]
5. Morgelin M, Paulsson M, Hardingham TE, Heinegard D, Engel J. Cartilage proteoglycans. Assembly with hyaluronate and link protein as studied by electron microscopy. *Biochem J.* 1988; 253:175–185. [PubMed: 3421941]
6. Neame PJ, Barry FP. The link proteins. *Experientia.* 1993; 49:393–402. [PubMed: 8500595]
7. Wirrig EE, Snarr BS, Chintalapudi MR, et al. Cartilage link protein 1 (Crtl1), an extracellular matrix component playing an important role in heart development. *Dev Biol.* 2007; 310:291–303. [PubMed: 17822691]
8. Auvinen P, Tammi R, Parkkinen J, et al. Hyaluronan in peritumoral stroma and malignant cells associates with breast cancer spreading and predicts survival. *Am J Pathol.* 2000; 156:529–536. [PubMed: 10666382]
9. Anttila MA, Tammi RH, Tammi MI, Syrjanen KJ, Saarikoski SV, Kosma VM. High levels of stromal hyaluronan predict poor disease outcome in epithelial ovarian cancer. *Cancer Res.* 2000; 60:150–155. [PubMed: 10646867]
10. Ropponen K, Tammi M, Parkkinen J, et al. Tumor cell-associated hyaluronan as an unfavorable prognostic factor in colorectal cancer. *Cancer Res.* 1998; 58:342–347. [PubMed: 9443415]
11. Boregowda RK, Appaiah HN, Siddaiah M, et al. Expression of hyaluronan in human tumor progression. *J Carcinog.* 2006; 5:2. [PubMed: 16401353]
12. Nara Y, Kato Y, Torii Y, et al. Immunohistochemical localization of extracellular matrix components in human breast tumours with special reference to PG-M/versican. *Histochem J.* 1997; 29:21–30. [PubMed: 9088942]
13. Lokeshwar VB, Obek C, Pham HT, et al. Urinary hyaluronic acid and hyaluronidase: markers for bladder cancer detection and evaluation of grade. *J Urol.* 2000; 163:348–356. [PubMed: 10604388]
14. Grammatikakis N, Grammatikakis A, Yoneda M, Yu Q, Banerjee SD, Toole BP. A novel glycosaminoglycan-binding protein is the vertebrate homologue of the cell cycle control protein, Cdc37. *J Biol Chem.* 1995; 270:16198–16205. [PubMed: 7608185]
15. Das S, Deb TB, Kumar R, Datta K. Multifunctional activities of human fibroblast 34-kDa hyaluronic acid-binding protein. *Gene.* 1997; 190:223–225. [PubMed: 9185871]
16. Huang L, Grammatikakis N, Yoneda M, Banerjee SD, Toole BP. Molecular characterization of a novel intracellular hyaluronan-binding protein. *J Biol Chem.* 2000; 275:29829–29839. [PubMed: 10887182]
17. Gunthert U, Hofmann M, Rudy W, et al. A new variant of glycoprotein CD44 confers metastatic potential to rat carcinoma cells. *Cell.* 1991; 65:13–24. [PubMed: 1707342]
18. Tammi MI, Day AJ, Turley EA. Hyaluronan and homeostasis: a balancing act. *J Biol Chem.* 2002; 277:4581–4584. [PubMed: 11717316]
19. Desai B, Rogers MJ, Chellaiah MA. Mechanisms of osteopontin and CD44 as metastatic principles in prostate cancer cells. *Mol Cancer.* 2007; 6:18. [PubMed: 17343740]
20. Wang SJ, Wreesmann VB, Bourguignon LY. Association of CD44 V3-containing isoforms with tumor cell growth, migration, matrix metalloproteinase expression, and lymph node metastasis in head and neck cancer. *Head Neck.* 2007; 6:550–558. [PubMed: 17252589]
21. Bourguignon LY, Peyrollier K, Gilad E, Brightman A. Hyaluronan-CD44 interaction with neural Wiskott-Aldrich syndrome protein (N-WASP) promotes actin polymerization and ErbB2 activation leading to β -catenin nuclear translocation, transcriptional up-regulation, and cell migration in ovarian tumor cells. *J Biol Chem.* 2007; 282:1265–1280. [PubMed: 17092940]
22. Li Y, Heldin P. Hyaluronan production increases the malignant properties of mesothelioma cells. *Br J Cancer.* 2001; 85:600–607. [PubMed: 11506502]
23. Thylen A, Wallin J, Martensson G. Hyaluronan in serum as an indicator of progressive disease in hyaluronan-producing malignant mesothelioma. *Cancer.* 1999; 86:2000–2005. [PubMed: 10570424]
24. Afify AM, Stern R, Michael CW. Differentiation of mesothelioma from adenocarcinoma in serous effusions: the role of hyaluronic acid and CD44 localization. *Diagn Cytopathol.* 2005; 32:145–150. [PubMed: 15690337]

25. Welker L, Muller M, Holz O, Vollmer E, Magnussen H, Jorres RA. Cytological diagnosis of malignant mesothelioma—improvement by additional analysis of hyaluronic acid in pleural effusions. *Virchows Arch.* 2007; 450:455–461. [PubMed: 17377812]
26. Attanoos RL, Webb R, Gibbs AR. CD44H expression in reactive mesothelium, pleural mesothelioma and pulmonary adenocarcinoma. *Histopathology.* 1997; 30:260–263. [PubMed: 9088956]
27. Tusher VG, Tibshirani R, Chu G. Significance analysis of microarrays applied to the ionizing radiation response. *Proc Natl Acad Sci U S A.* 2001; 98:5116–5121. [PubMed: 11309499]
28. Li J, Wong L. Emerging patterns and gene expression data. *Genome Inform.* 2001; 12:3–13. [PubMed: 11791219]
29. Lin M, Wei LJ, Sellers WR, Lieberfarb M, Wong WH, Li C. dChipSNP: significance curve and clustering of SNP-array-based loss-of-heterozygosity data. *Bioinformatics.* 2004; 20:1233–1240.
30. Lucito R, Healy J, Alexander J, et al. Representational oligonucleotide microarray analysis: a high-resolution method to detect genome copy number variation. *Genome Res.* 2003; 13:2291–2305. [PubMed: 12975311]
31. Ivanov SV, Miller J, Lucito R, et al. Identification of genomic events associated with progression of pleural malignant mesothelioma. *J Pathol.* 2008; 124:589–599.
32. Ivanov SV, Salnikow K, Ivanova AV, Bai L, Lerman MI. Hypoxic repression of STAT1 and its downstream genes by a pVHL/HIF-1 target DEC1/STRA13. *Oncogene.* 2007; 26:802–812. [PubMed: 16878149]
33. Pass HI, Stevens EJ, Oie H, et al. Characteristics of nine newly derived mesothelioma cell lines. *Ann Thorac Surg.* 1995; 59:835–844. [PubMed: 7695406]
34. Morgelin M, Heinegard D, Engel J, Paulsson M. The cartilage proteoglycan aggregate: assembly through combined protein-carbohydrate and protein-protein interactions. *Biophys Chem.* 1994; 50:113–128. [PubMed: 8011926]
35. Morgelin M, Paulsson M, Heinegard D, Aebi U, Engel J. Evidence of a defined spatial arrangement of hyaluronate in the central filament of cartilage proteoglycan aggregates. *Biochem J.* 1995; 307:595–601. [PubMed: 7733901]
36. Golshani R, Lopez L, Estrella V, Kramer M, Iida N, Lokeshwar VB. Hyaluronic acid synthase-1 expression regulates bladder cancer growth, invasion, and angiogenesis through CD44. *Cancer Res.* 2008; 68:483–491. [PubMed: 18199543]
37. Gotte M, Yip GW. Heparanase, hyaluronan, and CD44 in cancers: a breast carcinoma perspective. *Cancer Res.* 2006; 66:10233–10237. [PubMed: 17079438]
38. Peterson RM, Yu Q, Stamenkovic I, Toole BP. Perturbation of hyaluronan interactions by soluble CD44 inhibits growth of murine mammary carcinoma cells in ascites. *Am J Pathol.* 2000; 156:2159–2167. [PubMed: 10854236]
39. Silletti S, Yebra M, Perez B, Cirulli V, McMahon M, Montgomery AM. Extracellular signal-regulated kinase (ERK)-dependent gene expression contributes to L1 cell adhesion molecule-dependent motility and invasion. *J Biol Chem.* 2004; 279:28880–28888. [PubMed: 15128735]
40. Boo YJ, Park JM, Kim J, et al. L1 expression as a marker for poor prognosis, tumor progression, and short survival in patients with colorectal cancer. *Ann Surg Oncol.* 2007; 14:1703–1711. [PubMed: 17211730]
41. Matsumoto K, Shionyu M, Go M, et al. Distinct interaction of versican/PG-M with hyaluronan and link protein. *J Biol Chem.* 2003; 278:41205–41212. [PubMed: 12888576]
42. Seyfried NT, McVey GF, Almond A, Mahoney DJ, Dudhia J, Day AJ. Expression and purification of functionally active hyaluronan-binding domains from human cartilage link protein, aggrecan and versican: formation of ternary complexes with defined hyaluronan oligosaccharides. *J Biol Chem.* 2005; 280:5435–5448. [PubMed: 15590670]
43. Cavallaro U, Christofori G. Cell adhesion and signalling by cadherins and Ig-CAMs in cancer. *Nat Rev Cancer.* 2004; 4:118–132. [PubMed: 14964308]
44. Gilg AG, Tye SL, Tolliver LB, et al. Targeting hyaluronan interactions in malignant gliomas and their drug-resistant multipotent progenitors. *Clin Cancer Res.* 2008; 14:1804–1813. [PubMed: 18347183]

45. Ward JA, Huang L, Guo H, Ghatak S, Toole BP. Perturbation of hyaluronan interactions inhibits malignant properties of glioma cells. *Am J Pathol.* 2003; 162:1403–1409. [PubMed: 12707023]
46. Liu N, Lapcevich RK, Underhill CB, et al. Metastatin: a hyaluronan-binding complex from cartilage that inhibits tumor growth. *Cancer Res.* 2001; 61:1022–1028. [PubMed: 11221828]
47. Mohapatra S, Yang X, Wright JA, Turley EA, Green-berg AH. Soluble hyaluronan receptor RHAMM induces mitotic arrest by suppressing Cdc2 and cyclin B1 expression. *J Exp Med.* 1996; 183:1663–1668. [PubMed: 8666924]
48. Xu XM, Chen Y, Chen J, et al. A peptide with three hyaluronan binding motifs inhibits tumor growth and induces apoptosis. *Cancer Res.* 2003; 63:5685–5690. [PubMed: 14522884]

Translational Relevance

Malignant pleural mesothelioma (MPM) is a lethal asbestos-associated cancer with a short median survival and a high resistance to all types of conventional treatment. Developing effective diagnostic and therapeutic tools requires identification of novel early detection markers for MPM and understanding their significance for tumor initiation and growth. We have identified and validated that a novel link protein, hyaluronan- and proteoglycan-linked protein1 (HAPLN1), is overexpressed in MPM as opposed to lung cancer. HAPLN1 serves as a prognostic marker because its expression at higher levels in MPM patients is associated with a poor prognosis. Moreover, we have documented the protumorigenic role of HAPLN1 in MPM *in vitro* and identified the NH₂-terminal IgV domain as a promoter of tumorigenic activities for the HAPLN1 protein. These data support a central role for HAPLN1 in MPM progression and could stimulate interest in the development of novel targeted therapies against the IgV domain.

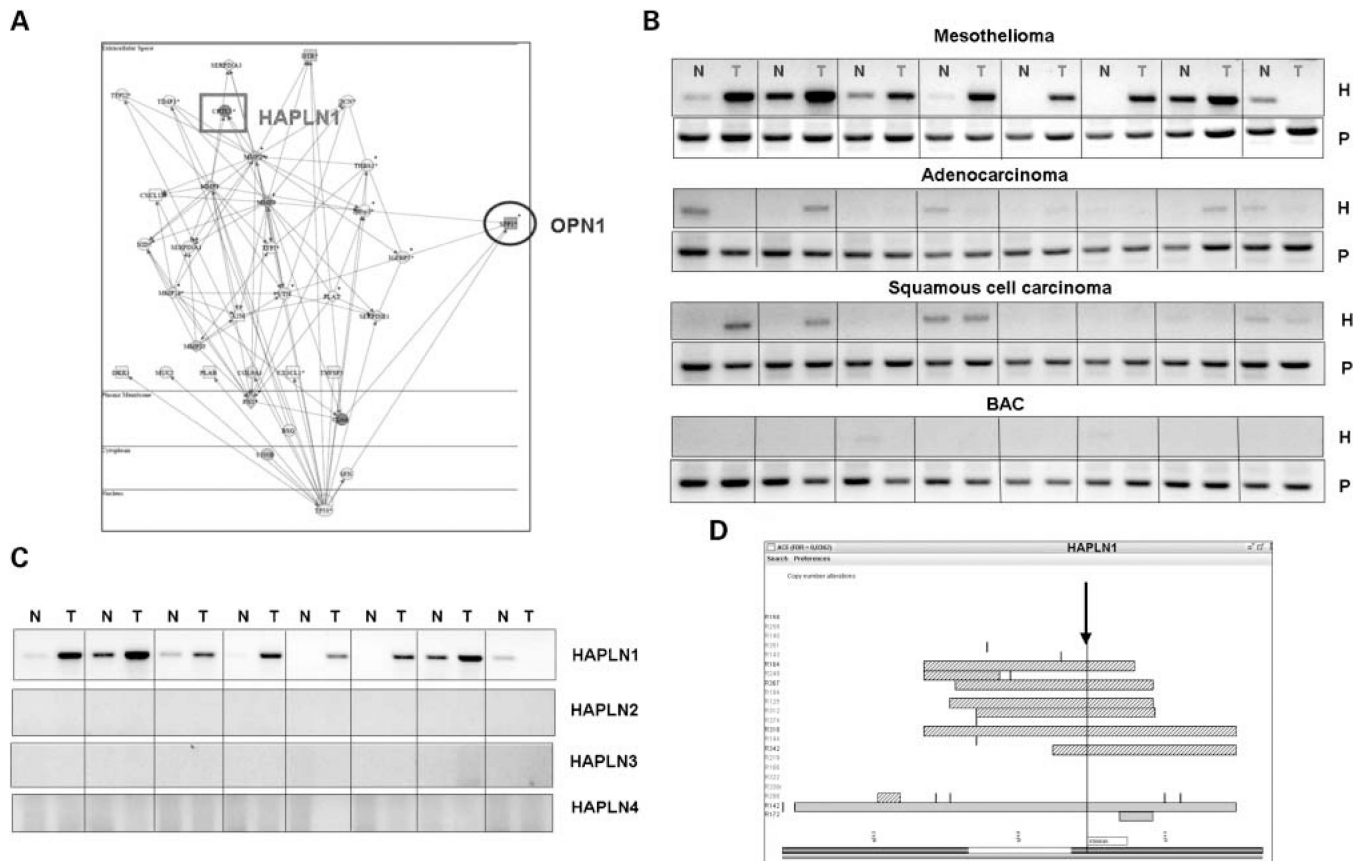


Fig. 1. HAPLN1 is highly expressed specifically in mesotheliomas. *A*, pathway analysis of highly expressed extracellular or secreted genes comparing peritoneum to early stages of MPM. Pathways analysis was done using Ingenuity software. Differential microarray analysis was done on Affymetrix chips. HAPLN1 and SPP1 [osteopontin (OPN1)] are marked. *B*, semiquantitative RT-PCR analysis of RNA isolated from matched normal and tumor samples of mesothelioma, lung adenocarcinoma, lung squamous cell carcinoma, and bronchioloalveolar carcinoma patients. *Top*, RT-PCR products obtained with the HAPLN1 specific primers; *bottom*, loading control, RT-PCR products with the primers specific for invariable gene PPIA. *N*, normal tissue; *T*, tumor. *C*, semiquantitative RT-PCR analysis of RNA isolated from eight matched normal/tumor pairs of mesothelioma with primers specific for four members of HAPLN gene family. *D*, analysis of genomic rearrangements in mesothelioma done by ROMA revealed frequent amplification of the HAPLN1 locus (5q14.3) in mesothelioma patients (false discovery rate = 0.036). *Arrow*, HAPLN1 locus; *hatched boxes*, amplifications in tumors compared with normal tissues. Patient samples are marked with R* numbers.

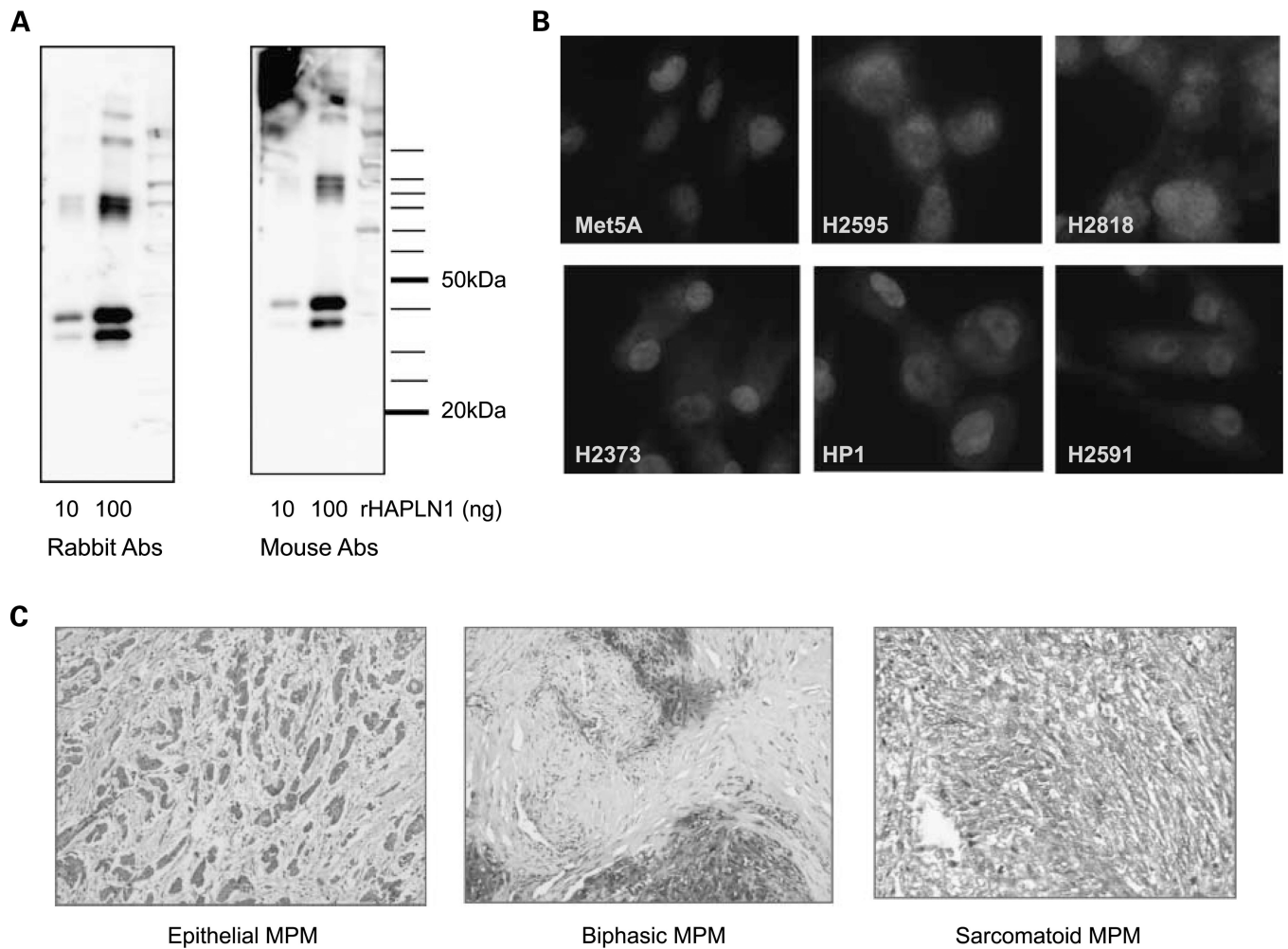


Fig. 2. HAPLN1 protein is a marker of mesothelioma cells and tumors. *A*, Western blot on recombinant human HAPLN1 protein with rabbit polyclonal and mouse monoclonal anti-HAPLN1. Both antibodies recognize HAPLN1-specific bands pattern, and 10 and 100 ng rHAPLN1 protein per lane was loaded. *B*, immunostaining of mesothelioma cells and immortalized normal mesothelial cells (Met5A) with rabbit polyclonal anti-HAPLN1 antibodies. *C*, immunohistochemical staining of different types of mesothelioma with rabbit anti-HAPLN1 antibodies (*top*).

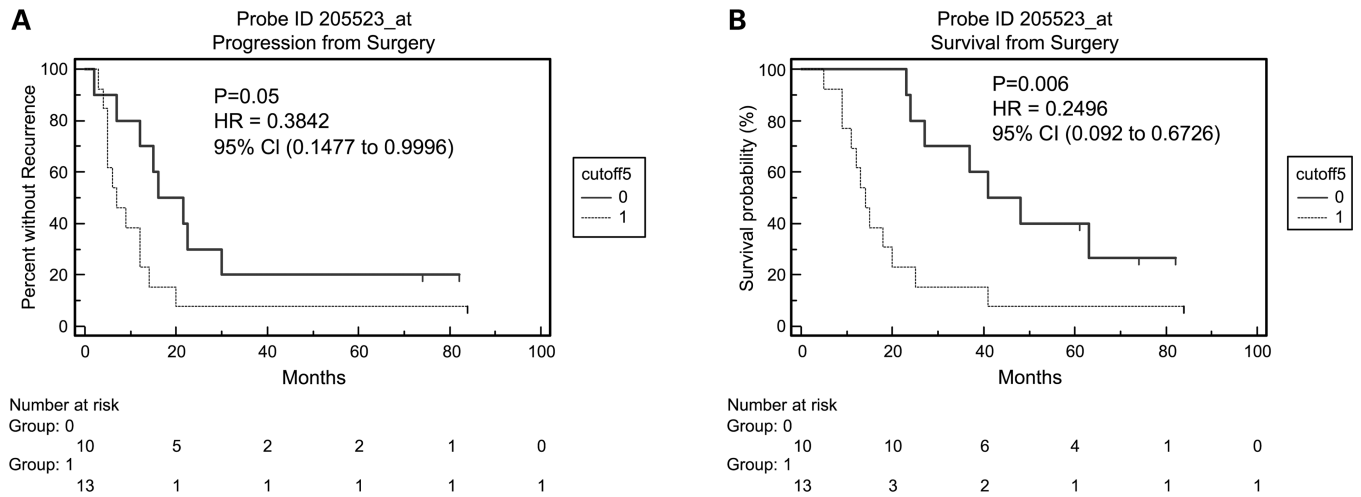


Fig. 3. Kaplan-Meier progression and survival estimates. Time to progression (*A*) and survival (*B*) after surgery was significantly worse in patients with tumors expressing HAPLN1 at high level than in patients with tumors with low or negative expression of HAPLN1. 0, low or no expression; 1, high expression. *CI*, confidence intervals; *HR*, hazard ratio.

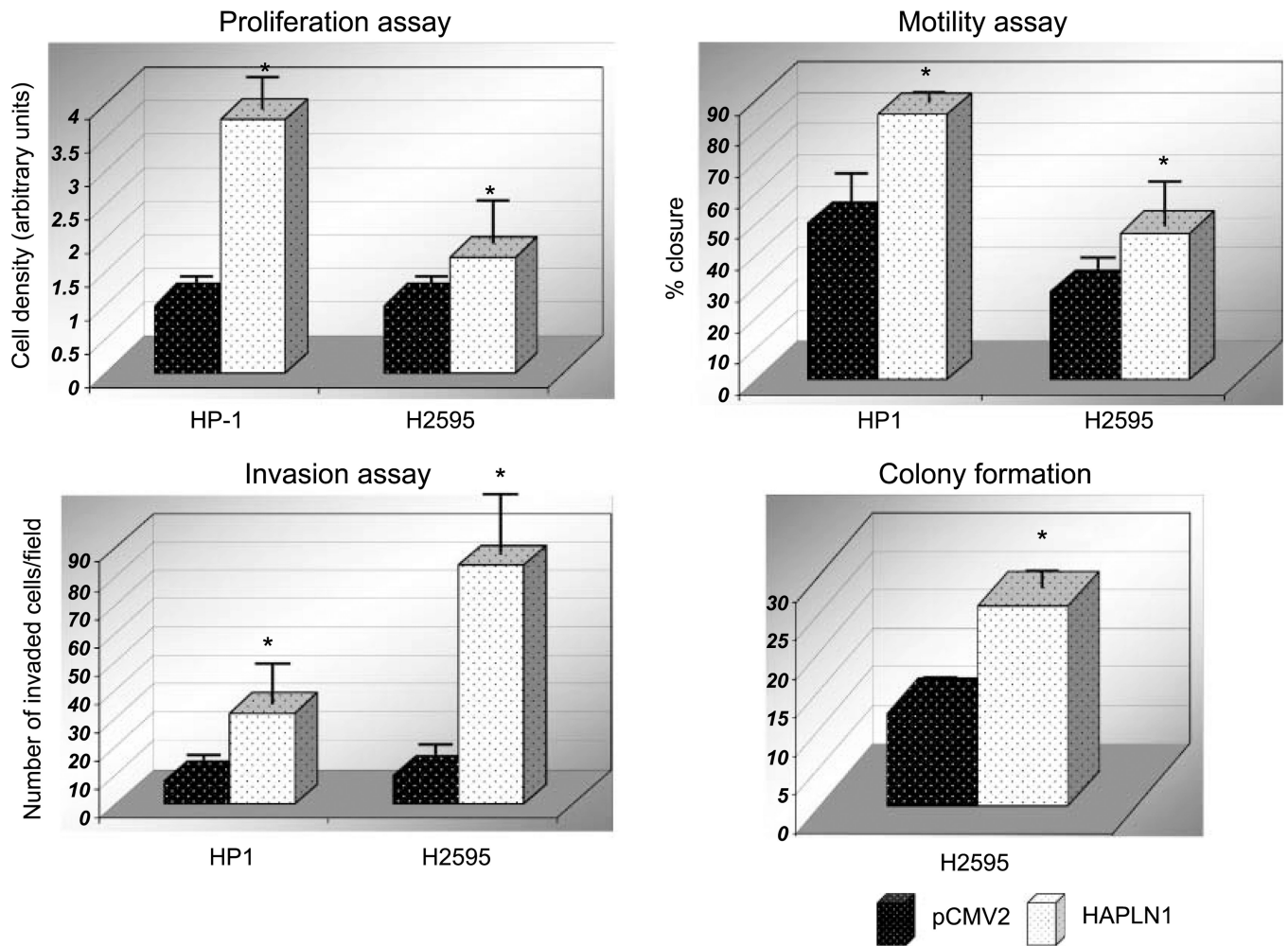


Fig. 4. HAPLN1 overexpression augments the tumorigenic potential of mesothelioma cells. HP1 and H2595 mesothelioma cells were transiently transfected with HAPLN1-expressing construct and mock vector and resulting cells were tested on proliferation, motility, invasion, and anchorage-independent growth. *Black*, control cells (pCMV2-transfected); *white*, HAPLN1-transfected cells. *Stars*, statistically significant difference.

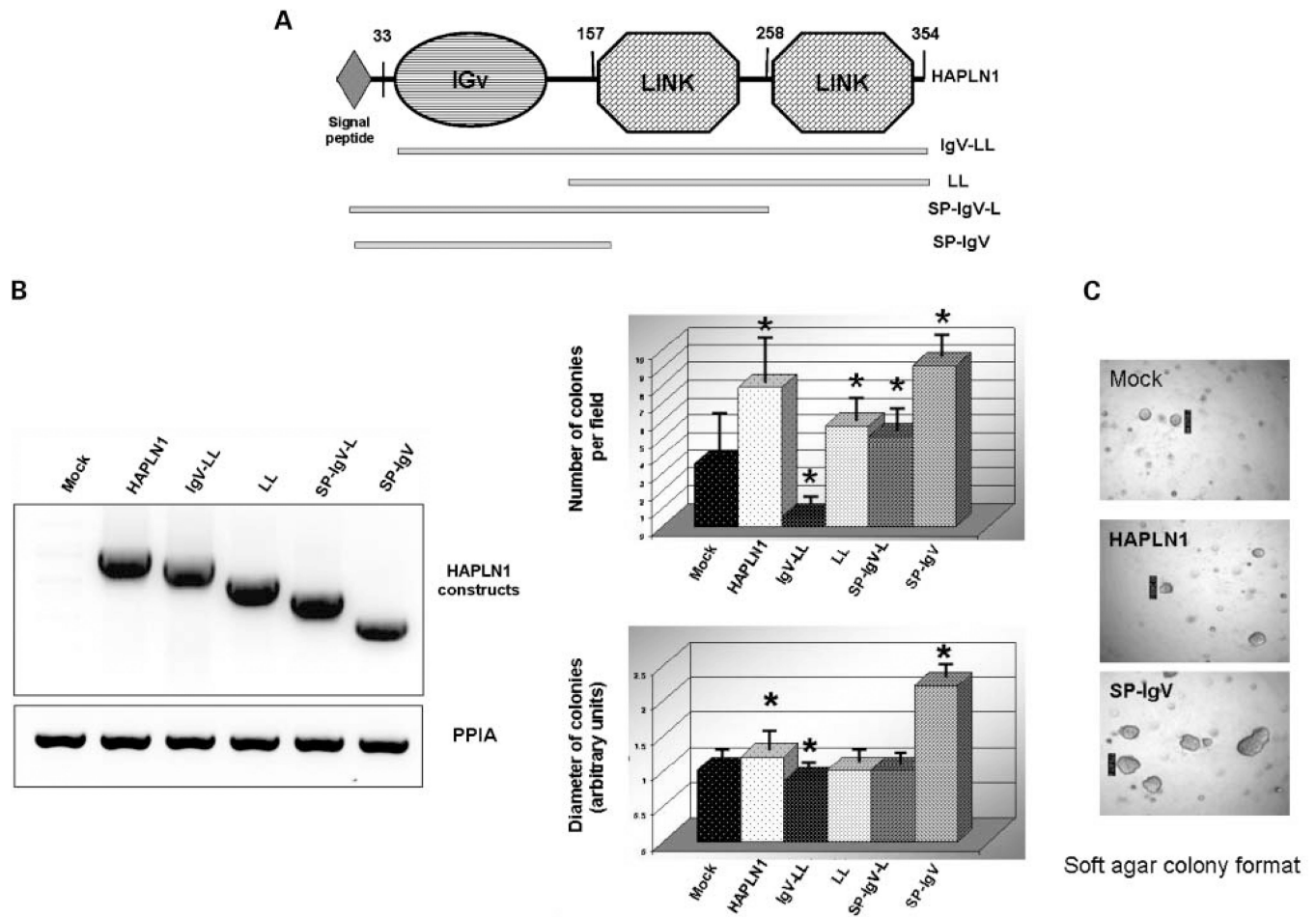


Fig. 5. Domains of the HAPLN1 protein play different roles in the tumorigenic potential of this protein. *A*, domain structure of the HAPLN1 protein and its deletion mutants. *SP*, signal peptide; *IgV*, immunoglobulin-like domain; *L*, link domain. *B*, RT-PCR analysis of HAPLN1 mutants in H2595-transfected cells. RT-PCR was done using primers specific to each HAPLN1 mutant. Products were separated by electrophoresis in 0.8% agarose gel and stained with ethidium bromide. Note the absence of HAPLN1 product in control cells. *Bottom*, expression of invariably expressed gene PPIA. *C*, effect of HAPLN1 deletion mutants on anchorage-independent growth of Hmeso cells as analyzed by soft-agar colony formation assay. Stars, statistically significant difference. *Right*, difference in colony size in control cells, cells transfected with HAPLN1 full-length construct, and cells transfected with the most tumorigenic SP-IgV mutant.

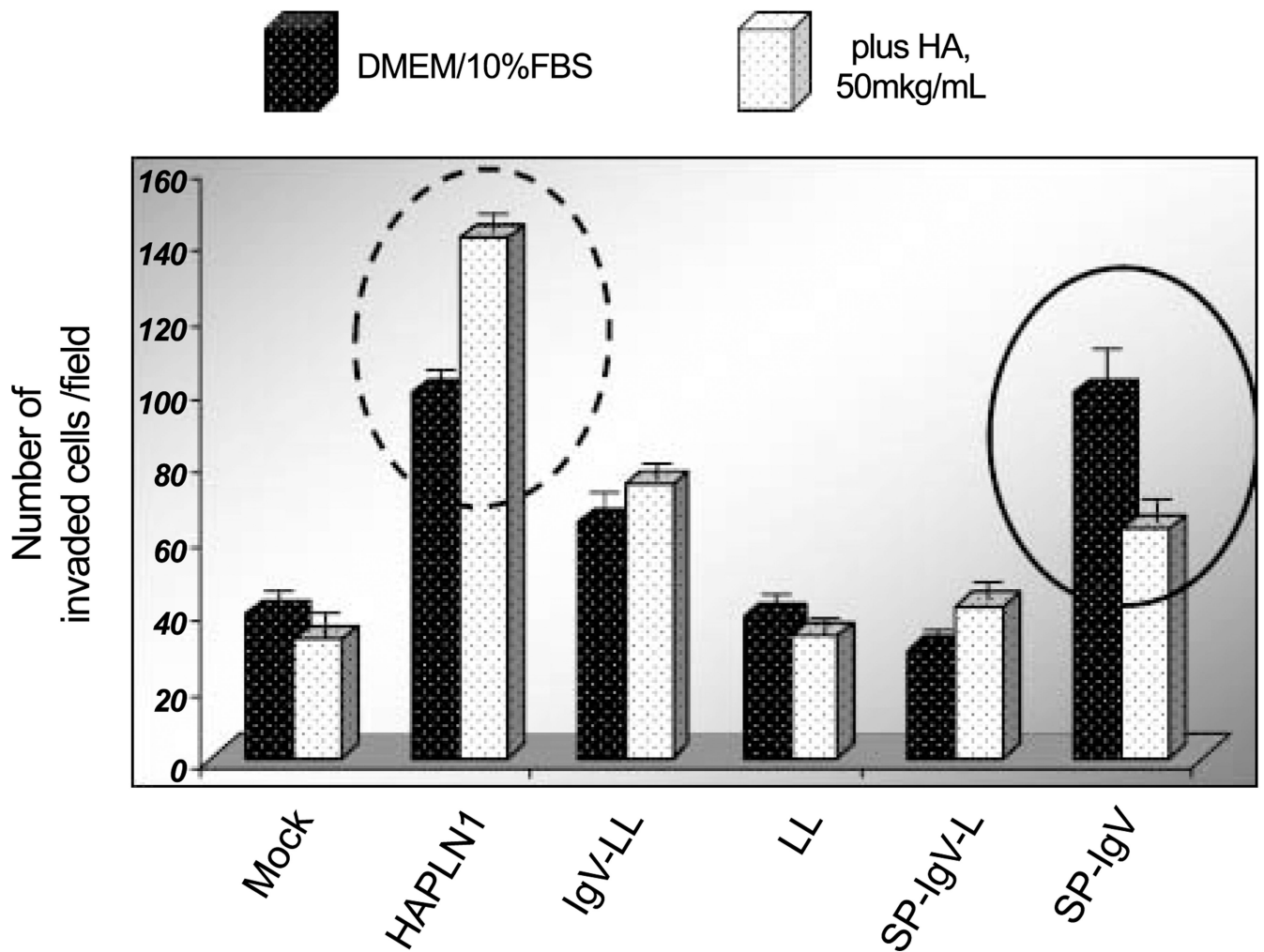


Fig. 6. Effect of HA on the invasion properties of mesothelioma cells transfected with HAPLN1 mutants. H2595 cells (2×10^5) were transfected with HAPLN1 deletion mutants and incubated in the presence or absence of 50 μ g/mL HA in 10% FBS/DMEM for 48 h. The number of cells invaded the reconstituted basement membrane matrix was calculated as described in Materials and Methods. Assays were done twice in triplicate. *Points*, mean of triplicates from two different experiments; *bars*, SD. Cells transfected with deletion mutants, except for LL, showed statistically significant difference compared with control cells. *Black columns*, regular medium; *white columns*, HA-supplemented medium.

Table 1

Results of scoring of tissue microarray slides containing 40 mesothelioma and 60 lung cancer samples stained with rabbit anti-HAPLN1 antibodies

Tumor cells reactive	Mesothelioma (n = 40)	Lung cancer (n = 60)
0	1	53
1–25%	0	0
25–50%	0	3
50–75%	8	3
>75%	31	1

Table 2

Effect of HAPLN1 deletion mutants on tumorigenic properties of MPM cells shown as a fold change between control MPM cells and MPM cells transfected with HAPLN1 deletion mutants

HAPLN1 mutant	Proliferation	Motility	Invasion	Invasion/HA	Colony number	Colony size
Full length	1.3*	3.3*	2.5*	4.4*	2.2*	1.2*
IgV-LL	1.05	2.2*	1.6*	2.3*	0.14*	0.8*
LL	0.87*	2.0*	1.0	1.0	1.6*	1.0
SP-IgV-L	1.04	1.9*	0.7*	1.3*	1.4*	1.0
SP-IgV	1.33*	2.9*	2.5*	1.9*	2.5*	2.2*

NOTE: All values in table expressed as fold change.

* Statistically significant difference.